EUROPEAN ORGANIZATION FOR NUCLEAR RESEARCH

CERN-EP/88-60
May 26, 1988

Evidence for Transverse Jets in High Mass Diffraction

(UA8 Experiment)

R. Bonino[1], A. Brandt, J. B. Cheze[2], S. Erhan, G. Ingelman[3],
M. Medinnis, P. E. Schlein, J. Zsembery[2], J. G. Zweizig
University of California[*)], Los Angeles, California 90024, USA.

A. G. Clark[4], J. R. Hansen[5]
CERN, 1211 Geneva 23, Switzerland.

Abstract

Localized energy clusters (jets) with transverse energy between 5 and 13 GeV are observed semi-inclusively in proton-antiproton interactions with $\sqrt{s} = 630$ GeV which also contain a final state proton with more than 90% of the beam proton's momentum. The system which recoils against the proton is studied for invariant masses in the range 105 to 190 GeV. The production rate, angular and energy distributions and profiles of the clusters are in good agreement with predictions of a QCD model of diffractive scattering, in which the clusters result from the hard scattering of gluons in an exchanged Pomeron with the partons in an incident proton. A soft gluon structure function of the Pomeron, such as $(1-x)^5$, is preferred.

Submitted to Physics Letters B

---

*) Supported by U.S. National Science Foundation grant PHY85-09175

[1]) now at INFN, Rome, Italy.
[2]) Centre d'Etudes Nucleaires-Saclay.
[3]) now at DESY, Hamburg, FRG.
[4]) now at Fermilab, Batavia, IL, USA.
[5]) now at Nils Bohr Institute, Copenhagen, Denmark

The observation of transverse energy clusters (jets) in high energy $\bar{p}p$[1,2] or pp[3,4] interactions provides clear evidence for the occurence of point-like scattering between constituents and is in quantitative agreement with calculations of quark and gluon scattering in QCD[5].

In this Letter, we report the first observation of localized transverse energy depositions (clusters) produced in the special class of events which contain a final state proton which possesses more than 90% of the beam proton momentum. The experiment was performed at the CERN SPS-Collider with $\sqrt{s}$ = 630 GeV. The final state proton in the reaction:

$$p\bar{p} \rightarrow pX \qquad (1)$$

is detected in the Roman pot spectrometer[6] of experiment UA8 in the same interaction region in which experiment UA2[1,7] is installed. This recoil proton spectrometer uses the quadrupole magnets of the SPS for momentum analysis of the high momentum protons in Reaction 1. The particle trajectory is measured by wire chambers installed in Roman pots which can be positioned near the SPS beams. The UA2 central calorimeter[7], shown in Fig. 1, covers the range of pseudo-rapidity $|\eta| < 1$ and is used to study the structure of the remaining event in the central region.

Events with elastic-like final state protons, called inelastic (single) diffraction[8], are believed to result from the dominant exchange of a color-singlet Pomeron. Inclusive measurements of Reaction 1 have previously been made at the SPS-Collider by Bozzo et al.[9]. In the kinematic range of the data in Ref. [9] and the data discussed in this Letter, the contribution of f-meson exchange should be less than a few percent[10].

In spite of the large cross section for diffractive processes, the nature of the exchanged Pomeron is far from being understood. It has been argued[11] that the observation of hard scattering effects in Reaction 1 would signal the occurance of perturbative QCD processes between the partons in one beam particle with partons in the Pomeron emitted from the other beam particle. The largest cross sections for such signals would be provided by the leading order QCD $2 \rightarrow 2$ scattering processes which result in the emission of clusters of particles (jets) which possess large transverse energy, E_t. With sufficient data, the study of such events should lead to a detailed understanding of the internal structure of the Pomeron[11]. A background to diffractive jet production given by normal high-p_t scattering, where a spectator parton fragments into a leading proton that mimics the diffractive signature, has been estimated[12] to have at least two orders-of-magnitude smaller cross section and can therefore be neglected.

To search for jet structure in the diffractive system, X, of Reaction 1, we constructed a trigger which required a coincidence between scintillation counters mounted with each of three wire chambers in the Roman pot spectrometer and a total transverse energy, $\Sigma E_t > 9$ GeV, measured[1] in the UA2 central calorimeter system[7]. The calorimeter is segmented into 240 cells, each covering 15^0 in ϕ and 10^0 in θ, and built in a tower structure pointing to the center of the interaction region. The polar angle range is: $40^0 < \theta < 140^0$. The trigger initiated a readout of both the UA2 detector and the recoil proton spectrometer for logging by the UA2 data acquisition system concurrently with normal UA2 events. Data were also recorded with an inclusive proton trigger, which was identical to the trigger described above except that no demands were made on ΣE_t. The results presented here were obtained in a short run with an integrated luminosity of 11 nb^{-1} in December 1985.

Each chamber in the Roman pot spectrometer contains 6 planes with 2 mm wire spacing. There are two planes with horizontal wires, y and y′ shifted half a cell, and two sets of $\pm 7^0$ stereo views, u − u′ and v − v′. With a 4-bit time-to-digital converter on each wire, a chamber provides about 55 μm position resolution in the vertical (bending) plane. The final state proton momentum is calculated using the vertex position of the event given by the UA2 central chamber system and points reconstructed from hits in chambers 1 and 2; chamber 3 was used to check consistency.

---

[1] Despite the fact that a 9 GeV threshold was used in the online trigger for the data discussed here, the offline calibrated ΣE_t distribution showed no inefficiency at this value. Therefore, a cut of $\Sigma E_t > 9$ GeV was made in the offline analysis.

Fig. 2 shows the proton momentum measured with and without requiring an elevated ΣE_t in the trigger. When ΣE_t is included in the trigger requirements, the peak shifts to lower momentum, corresponding to larger values of diffractive mass M_X in Reaction 1, and a striking lower momentum enhancement develops which extends down to a proton Feynman-x, $x_p \approx 0.9$ ($M_X \approx 200$ GeV). The cutoff of this inclusive proton momentum distribution on the low side is an artifact of the apparatus acceptance.[2] For the high mass diffractive events discussed in this Letter the momentum transfer, t, to the recoil proton is approximately in the range[13], $1-2$ GeV^2.

For the data discussed here, the angular acceptance of the UA2 central detector, shown in Fig. 1, limits the jet acceptance to most of one hemisphere in the Pomeron-proton center-of-mass. A consequence of this acceptance limitation is that less than 10% of the events with one jet in the central calorimeter also have a second jet accepted. However, since the observable hemisphere is in the direction of the Pomeron, the observed single jet distributions are sensitive to the hardness of the Pomeron structure, as was pointed out in Ref. [11].

In the analysis which follows, we compare the experimental results with the model described in Ref. [11] in which the Pomeron is assumed to be a purely gluonic object with possible gluon structure functions, $xG(x) = 6(1-x)^5$ or $6x(1-x)$. In each case, x is the fraction of the Pomerons's momentum carried by the gluon. The jet production in the Pomeron-proton interaction is calculated from standard QCD $2 \rightarrow 2$ parton scattering matrix elements using a Monte Carlo event generator based on this model and with the hadronization described by the Lund model[14] and its Monte Carlo programs[15, 16]. Initial and final state parton radiation is taken into account as in Ref. [15], but produces no large effects at these relatively small momentum transfers. The generated Monte Carlo events are passed through a UA2 detector simulation program and data analysis software in order to subject the Monte Carlo events to the same biases as the real data.

We employ a cluster finding algorithm in which the calorimeter cell with largest transverse energy (required to be > 1.5 GeV) serves as an "initiator" cell. The transverse energies of all cells within a cone of radius $R = \sqrt{(\Delta\eta^2 + \Delta\phi^2)} = 1$ around the direction of the initiator cell are summed and, if larger than 5 GeV, accepted as a cluster.[3] Fig. 3 shows the distribution of the transverse energies of such clusters found in 114 events. Although the process was iterated to find all clusters in each event, only 7 of the events were found to possess a second cluster, in agreement with the expected number of two jet events in the sample. The solid curve in Fig. 3, normalized to the data, shows the predictions from the QCD model[11] discussed above and illustrates that the dependence on jet energy is as expected from hard scattering at the parton level. Within the quoted experimental errors, the shape of the Monte Carlo curve does not depend significantly on the exponent of the assumed structure function. The more difficult comparison of the absolute production rates of the clusters in the data and model is discussed below after comparing their other properties.

The energy profiles in polar (θ) and azimuthal (ϕ) angle, shown in Fig. 4(a-d), display the average shape of the clusters. Due to the limited calorimeter acceptance in θ, only events with $\theta_{jet} > 110^0$ are plotted on the θ plots, so that the energy flow on one side of the cluster axis can be observed in an unbiased way over a θ range larger than the cluster width. The widths, in both θ and ϕ, are seen to be in good agreement with the Monte Carlo events which embody the Lund model[14] prescription for fragmentation of high-E_t jets, known to be in agreement with the results of other jet production experiments[20,17]. We therefore conclude that our reconstructed energy clusters show typical jet properties.

---

[2] In future running of experiment UA8, this cutoff point occurs at much smaller momentum values, due to a reinstallation of some of the Roman pots closer to the interaction region. The acceptance of the UA2 calorimeter system has also been extended down to about 6^0 from the beam axis on both arms.

[3] Similar algorithms have been used by both the UA1[17] and UA2[18] collaborations. See also the discussion in Ref. [19].

It is interesting to note that the laboratory angular distribution of the 5-13 GeV jets found in the Lund Monte Carlo events used in our analysis is observed to be well correlated with the scattered parton directions on an event by event basis. Thus, at the Monte Carlo level, fluctuations can be ruled out as a source for the low energy jets considered here.

An additional argument that our 5-13 GeV transverse energy clusters are QCD jets and not due to fluctuations in low-p_t interactions comes from a comparison between the rates of cluster formation in our data and in Lund minimum bias Monte Carlo events, which satisfactorily describe minimum bias interactions up to Collider energies[21]. In our data , 26% of the events with $\Sigma E_t > 9$ GeV are found to possess a cluster with $E_t > 5$ GeV, whereas the corresponding number is only 2.8% for Monte Carlo events with the same mass (after removing events with scattered parton transverse momenta larger than 2.5 GeV, which are seen to correlate directly with the production of jets). In making this comparison, we assume that the Pomeron-proton interaction is similar to pp and $\bar{p}p$ interactions at the same $\sqrt{s}$. This seems reasonable in view of the similarity of the rapidity shapes of diffractive states and minimum bias events, as shown by the UA4 Collaboration[22]. We also note that clusters in the same range of E_t as ours have been observed in minimum bias events by the UA1 collaboration[23] and found to be in good agreement with jet production in QCD, whereas clusters which are statistical fluctuations in Monte Carlo events generated with non-QCD based models are too low in rate to agree with the data.

If our transverse energy clusters do indeed arise from hard parton scatterings, their longitudinal momenta in the Pomeron-proton cms should reflect the parton momenta in the Pomeron and, therefore, the hardness of its effective structure function[11]. Figs. 5[a-d] show the distributions in x_F (the cluster's longitudinal momentum normalized to 1/2 the diffractive mass, M_X) for three regions of M_X. As explained above, there is non-zero acceptance in only one hemisphere, which is in the direction of the incident Pomeron.

The curves in Figs. 5(a-d), normalized to the data, are the predictions of the model in Ref. [11] in which the exchanged Pomeron has beam momentum fractions of 0.034, 0.050 and 0.080, respectively (corresponding to the diffractive masses of 115, 140 and 170 GeV). The Pomeron is assumed to be a purely gluonic object with possible gluon structure functions,[4] $xG(x) = 6(1-x)^5$ or $6x(1-x)$. In each case in Figs. 5, the softer structure function, $(1-x)^5$, is preferred. This is summarized in Fig. 5(d), which shows the combined data for $x_{\bar{p}} = 0.91-0.972$. The curves in Fig. 5(d) have a χ^2/Degree of Freedom of 13.4/12 and 40.6/12, for the soft and hard structure functions, respectively.

Another characteristic feature of hard scattering processes which is sensitive to the Pomeron's structure is the laboratory angular distribution, θ, of the produced jets. Figs. 5(e-h) shows these distributions for the same $x_{\bar{p}}$ ranges as in Figs. 5(a-d). With the quasi-elastic protons observed at 0^0, the jet directions peak closer to 140^0, or larger opposite rapidity[8], at smaller diffractive masses. The falloff of the distributions near 140^0 in each plot is due to the loss in jet acceptance near the edge of the calorimeter. In each case, the solid and dashed curves, normalized to the data as before, are the predictions for the two Pomeron structure functions. The conclusions here are essentially the same as in the previous paragraph, namely that the $(1-x)^5$ structure function is preferred. We also note that the large asymmetry seen in Fig. 5(e) is a clear demonstration that our data sample does not contain any significant background from "pileup" events (i.e. accidental coincidences in the same machine bunch crossing between diffractive events and minimum bias events).

Concerning the rate of jet production, we use Equation 2 from Ref. [11]:

---

[4] The alternative hard structure function, $xG(x) = 2(1-x)$, gives results essentially indistinguishable from those of $6x(1-x)$ in Fig. 5 and is therefore not explicitly shown. This is a consequence of the fact that the jets under study mainly arise from the larger x part of the structure functions.

$$\frac{\Delta\sigma(\text{s.d.} \rightarrow \text{jets})}{\Delta\sigma(\text{s.d.} \rightarrow \text{all})} = \frac{\sigma(\text{Pp} \rightarrow \text{jets})}{\sigma(\text{Pp} \rightarrow \text{all})} \qquad (2)$$

rewritten so that the left-hand side is the observed fraction of diffractive events in a given bin of mass, M_X, and momentum transfer, t, which have clusters with $E_t > 5$ GeV. Assuming the validity of factorization in diffractive processes as in Ref. [11], this ratio is given by the fraction of Pomeron-proton interactions which yield jets, as shown on the right-hand side of Equation 2. The numerator, $\sigma(\text{Pp} \rightarrow \text{jets})$, is obtained from the QCD calculation discussed above, multiplied by the fraction of corresponding Monte Carlo events whose jets are detected by the calorimeter. In the denominator the Pomeron-proton total cross section, $\sigma(\text{Pp} \rightarrow \text{all})$, is taken to be 2.3 mbarn, as obtained from a triple-Regge analysis[24] of single diffractive data. It should be noted, however, that this value was determined for much smaller diffractive masses (< 10 GeV) than considered here and the assumption of a mass-independent value may not be correct.

In using Eq. 2 to compare data with predictions, we note that the proton acceptance efficiencies are identical in both numerator and denominator on the left hand side and therefore cancel. Furthermore, as mentioned, the same jet acceptance biases are imposed on both data and Monte Carlo events (the numerators on left and right hand sides, respectively). Thus, their comparison is meaningful, even though their absolute magnitudes are affected. We also note that because our Monte Carlo events model the data reasonably well, the conclusions of this paper are essentially independent of the parameters used in the jet finding algorithm.

Fig. 6 shows the three experimental values of the left hand side of Eq. 2 at the same x_p values used in Fig. 5, as well as the predictions corresponding to the right hand side of Eq. 2. The results are in agreement with our earlier conclusions. In particular, the rate comparison for the hard structure function is very poor whereas the soft structure function calculation is in reasonable agreement with the data, especially if one takes into account the limitation in our knowledge of $\sigma(\text{Pp} \rightarrow \text{all})$. In particular, we note that a $\sigma(\text{Pp} \rightarrow \text{all})$ which rises with increasing diffractive mass would tend to lower the curves as one goes from larger to smaller x_p in Fig. 6. However, a more precise determination of the shapes of the curves in Fig. 6 must await knowledge of the mass dependence of the Pomeron-proton total cross section from more detailed measurements and analysis of high mass diffractive data.

The curves in Fig. 6 assume that the Pomeron has a purely gluonic structure. A quark component with similar structure functions would yield lower rates due to smaller QCD parton level cross-sections. Donnachie and Landshoff[25] have recently proposed a model in which the hard scattering of a Pomeron is quark dominated with a structure function of the form $x(1-x)$ and with a normalisation of the momentum sum rule integral of $10-15\%$. Although the data in Figs. 5,6 can accomodate such a quark component, it is not sufficient in itself to account for the observed rate of jet production.

Concerning the absolute vertical scale in Fig. 6, we estimate that a multiplicitive factor of about 7 would correct for jet acceptance losses due to geometrical and detector resolution effects. This gives a jet production rate of about $10-15\%$ in our highest mass region. It is interesting to note that this is comparable to the rate inferred from the UA1 Collaboration study[23] of $\bar{p}p$ minimum bias interactions with $\sqrt{s} = 200$ GeV using the same jet definition parameters.

In summary, clusters with transverse energy in the range 5-13 GeV are observed in high mass diffractive final states. These show typical jet properties in agreement with other experiments and with theoretical expectations based on jet models. We have found no explanation of the effects in terms of fluctuations in low-p_t interactions. However, good agreement in all variables is obtained with a hard scattering model which is based on a gluon-dominated Pomeron with an effective gluon structure function of a rather soft nature, e.g. of the type $xG(x) = 6(1-x)^5$. Future analyses of higher statistics data from experiment UA8 will furnish more reliable absolute cross sections. In addition, we will be able to determine the dependence of the Pomeron's effective structure function on mass and momentum transfer.

The UCLA group is indebted to Pierre Darriulat, Luigi Di Lella, Peter Jenni and the entire UA2 collaboration for their very generous help and cooperation in making this run possible. We thank David Plane for his collaboration in the planning stages of the experiment. The support of the CERN administration is gratefully acknowledged.

References

[1] M. Banner et al, UA2 collaboration, Phys. Lett. B118 (1982) 203;
J.A. Appel et al., Phys. Lett. B160 (1985) 349.

[2] G. Arnison et al., UA1 Collaboration, Phys. Lett. B123 (1983) 115; Phys. Lett. B172 (1986) 461.

[3] T. Akesson et al., AFS Collaboration, Phys. Lett. B118 (1982) 185, 193.

[4] A.L.S.Angelis et al., CMOR Collaboration, Nucl. Phys. B244 (1984) 1.

[5] For example, see the review by: L. DiLella, Ann. Rev. Nucl. Part. Sci. 35 (1985) 107.

[6] J.G. Zweizig et al., Nucl. Instrum. and Meth. in Phys. Research A263 (1988) 188.

[7] A. Beer et al., Nucl. Instrum. Methods 224 (1984) 360.

[8] For reviews, see e.g.:
K. Goulianos, Phys. Rep. 101 (1983) 169;
G. Alberi and G. Goggi, Phys. Rep. 74 (1981) 1;
U. Amaldi, M. Jacob and G. Matthiae, Ann. Rev. Nucl. Sci. 26 (1976) 385.

[9] M. Bozzo et al., UA4 Collaboration, Phys. Letters B136 (1984) 217.

[10] A. Donnachie and P.V. Landshoff, Nucl. Phys. B244 (1984) 322.

[11] G. Ingelman and P.Schlein, Phys. Letters 152B (1985) 256.

[12] G. Ingelman, CERN-EP/85-159 and Proceedings of Workshop on Elastic and Diffractive Scattering at the Collider and Beyond, Blois, France (June 1985). Eds. B. Nicolescu, J. Tran Than Van (Editions Frontiers), page 135.

[13] see, for example, Fig. 19 in: P. Schlein, Proceedings of the XXIII International Conference on High Energy Physics, Berkeley, CA (16 – 23 July 1986), p. 1331.

[14] B. Andersson, G. Gustafson, G. Ingelman, T. Sjostrand, Phys. Rep. 97 (1983) 31.

[15] H.-U. Bengtsson, G. Ingelman, Comput. Phys. Commun. 34 (1985) 251;
H.-U. Bengtsson, T. Sjostrand, Comput. Phys. Commun. 46 (1987) 43.

[16] T. Sjostrand, Comput. Phys. Commun. 39 (1986) 347;
T. Sjostrand and M. Bengtsson, Comput. Phys. Commun. 43 (1987) 367.

[17] G. Arnison et al., UA1 Collaboration, Nucl. Phys. B276 (1986) 253;
F. Ceradini, UA1 Collaboration, Proceedings of the XXIII International Conference on High Energy Physics (Berkeley, 16-23 July, 1986) 1051.

[18] R. Ansari et al., UA2 Collaboration, Phys. Lett. B194 (1987) 158.

[19] The LHC Jet Study Group, T. Akesson et al., Report ECFA 84/85, CERN 84-10 (5 September, 1984).

[20] P. Bagnaia et al., UA2 Collaboration, Phys. Letters 144B (1984) 291;
T. Akesson et al., AFS Collaboration, Z. Phys. C30 (1986) 27;
P. Ghez and G. Ingelman, Z. Phys. C33 (1987) 465.

[21] T. Sjostrand and M. van Zijl, Phys. Rev. D36 (1987) 2019.

[22] D. Bernard et al., Phys. Letters 166B (1986) 459.

[23] C. Albajar et al., UA1 Collaboration, CERN-EP/88-29.

[24] E.L. Berger, J.C. Collins, D.E. Soper and G. Sterman, Nucl. Phys. B286 (1987) 704;
R.D. Field and G. Fox, Nucl. Phys. B80 (1974) 367;
R.L. Cool et al., Phys. Rev. Letters 47 (1981) 701.

[25] A. Donnachie and P. Landshoff, MC TH87/05 DAMTP 87/16 and Nucl. Phys. B (to be published).

Table 1: Event Sample

x_p of proton	Mean Diffractive Mass	Number of Events All	with jets > 5 GeV	single diffractive	$\frac{\Delta\sigma(\text{s.d.} \to \text{jets})}{\Delta\sigma(\text{all s.d.})}$
0.91 − 0.94	170 GeV	143(a)	37(a)	37(b)	0.0180 ± 0.0041
0.94 − 0.96	140 GeV	169	38	47	0.0141 ± 0.0031
0.96 − 0.972	115 GeV	156	39	66	0.0106 ± 0.0036

(a) trigger required $\Sigma E_t > 9$ GeV. $\int \mathscr{L} dt = 11.2$ nbarn^{-1}.
(b) no ΣE_t requirement in the trigger. $\int \mathscr{L} dt = 0.202$ nbarn^{-1}.

Figure Captions

1. UA2 Central Calorimeter. The recoil protons are measured in a Roman pot spectrometer as described in Ref. 6. The vectors show that the antiproton interacts with a $(1 - x_p)$ component of the incident proton. Thus interacting systems with lower mass move to the left with larger momentum.

2. Measured proton momentum distribution with and without the transverse energy requirement in the UA2 central calorimeter. The ordinate refers to the solid histogram. The dashed histogram is normalized to the other at its peak.

3. Raw jet energy distribution from events with $0.91 < x_p < 0.972$, for which $\Sigma E_t > 9$ GeV is required. The solid curve is the prediction from the model of Ref. [11] and is normalized to the data.

4. Jet energy profiles in θ and ϕ for events with $0.94 < x_p < 0.96$. (a) θ Distribution. Only jets whose axes have $\theta > 110^0$ are plotted in order to display the profile over a large range of θ. For each θ bin, the energies in all ϕ cells with that θ are summed. The ordinate is the average energy per event in a $\Delta\theta = 10^0$ cell. The dots show the data and the histograms show the same quantity for the Monte Carlo events generated according to the model described in the text. (b) shows the same quantity, but only adding those calorimeter cells which are within $|\Delta\phi| < 30^0$ from the jet axis. This is seen to greatly suppress the background from the underlying event. (c) ϕ Distribution. The ordinate is the average energy per event in a $\Delta\phi = 15^0$ cell. (d) same as (c), but only for those cells with $|\Delta\theta| < 20^0$.

5. (a-c)Distributions of Jet longitudinal momentum (normalized to $M_X/2$) in the center-of-mass of the diffractive system, X, for the 3 indicated ranges of x_p. In each case, the ordinate is (1/Number of Events)dN/dx_F. The solid and dashed curves, with the same normalization, show the distributions of the Monte Carlo events generated according to the structure functions $xG(x) = 6(1-x)^5$ and $6x(1-x)$, respectively, and passed through the UA2 detector simulation program, as discussed in the text. (d) The sum of (a-c) with the same normalization; (e-h) Distributions of laboratory angle, θ, of the jet axis for the same x_p selections as in (a-d).

6. Normalization comparison. The data points, given in Table I, correspond to the left-hand side of Eq. 2. The curves correspond to the right-hand side of Eq. 2, with the numerator generated for both structure functions. As discussed in the text, for the purpose of this figure, $\sigma(Pp \to \text{all})$ is taken to be constant at 2.3 mbarn over the entire range of x_p.

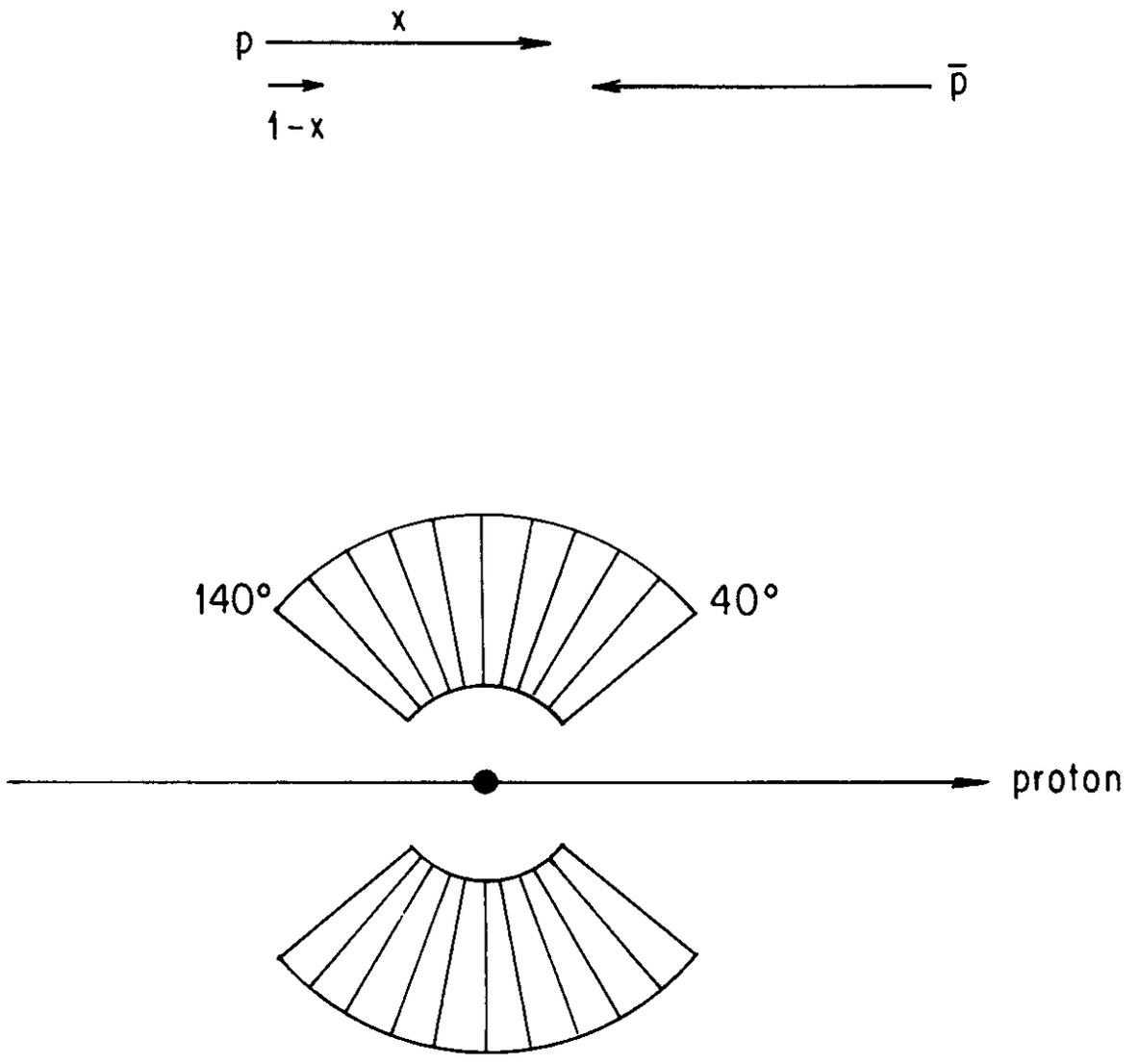

Fig. 1

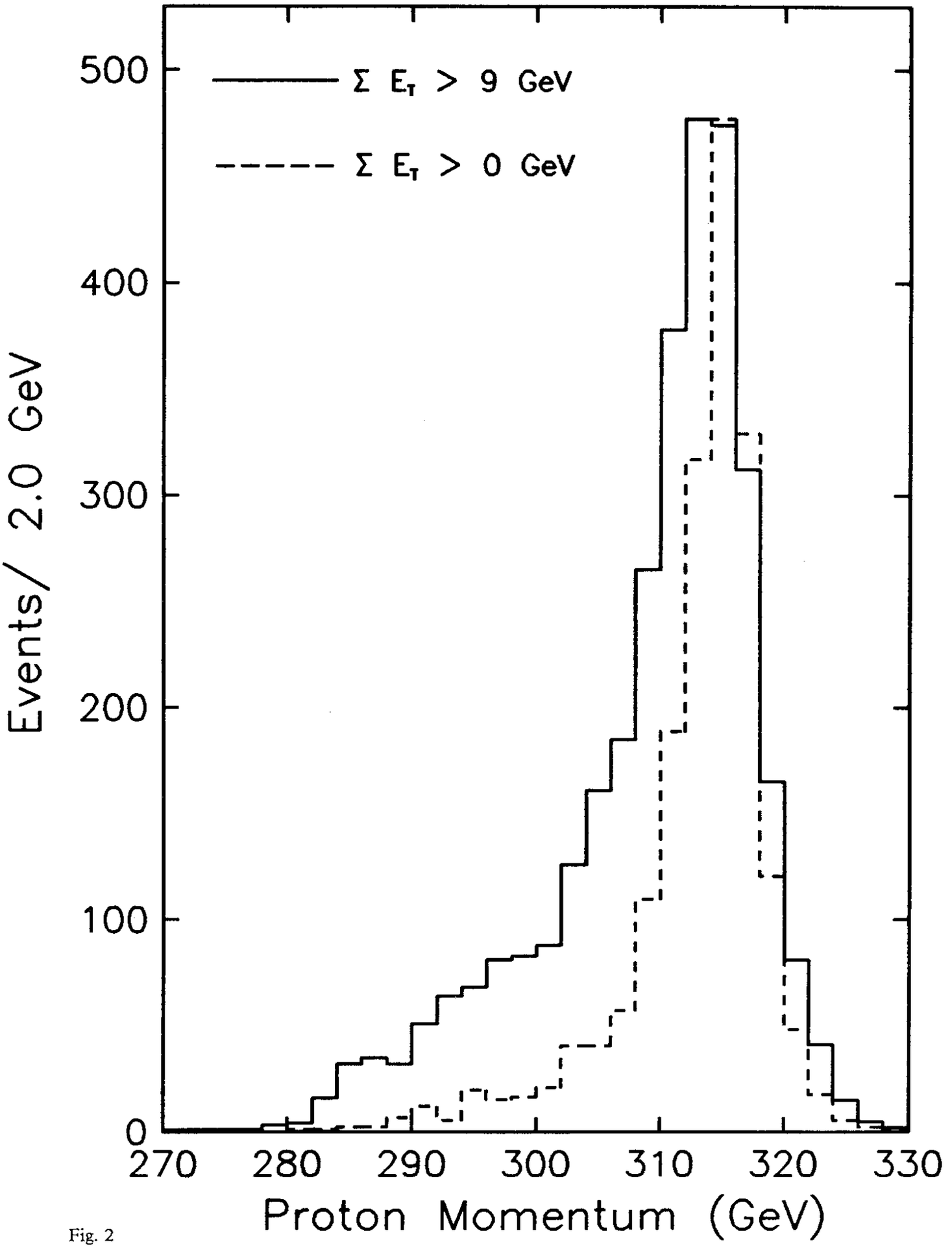
Σ E_T > 9 GeV
Σ E_T > 0 GeV
Events/ 2.0 GeV
0
100
200
300
400
500
270
280
290
300
310
320
330
Proton Momentum (GeV)

Fig. 2

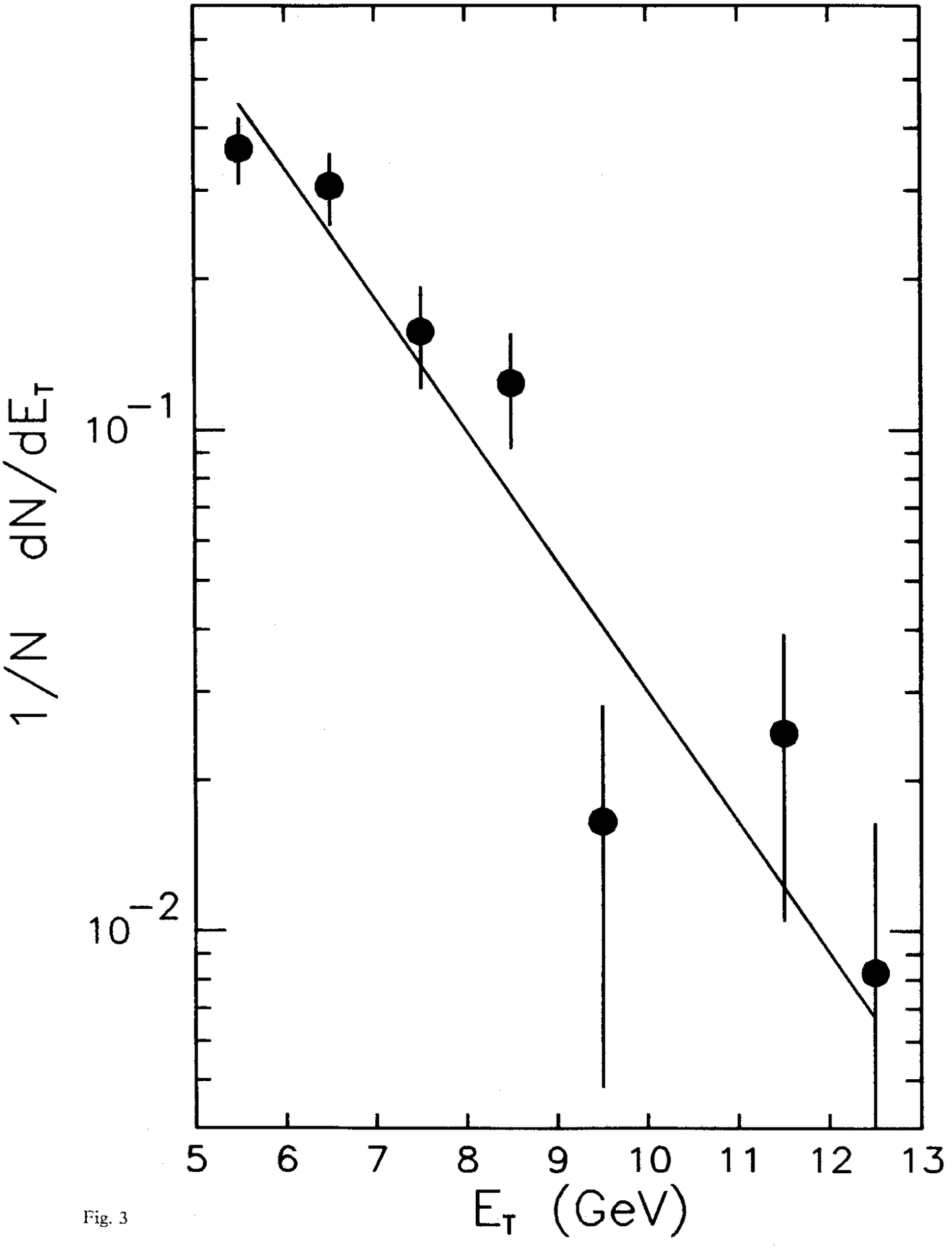

Fig. 3

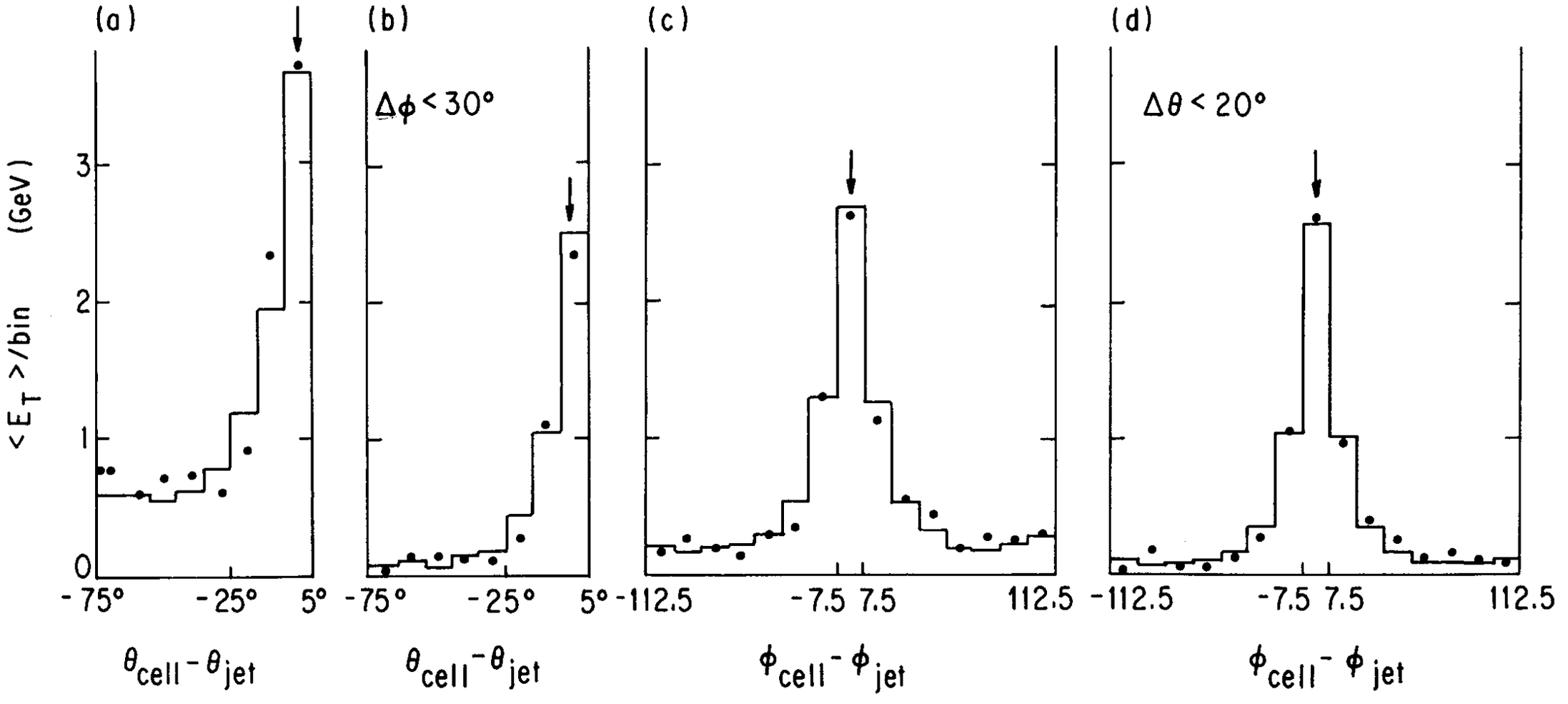
(a)
(b)
(c)
(d)
$\Delta\phi < 30°$
$\Delta\theta < 20°$
$\langle E_T \rangle$/bin (GeV)
0
1
2
3
-75°
-25°
5°
-112.5
-7.5
7.5
112.5
$\theta_{cell} - \theta_{jet}$
$\phi_{cell} - \phi_{jet}$

Fig. 4

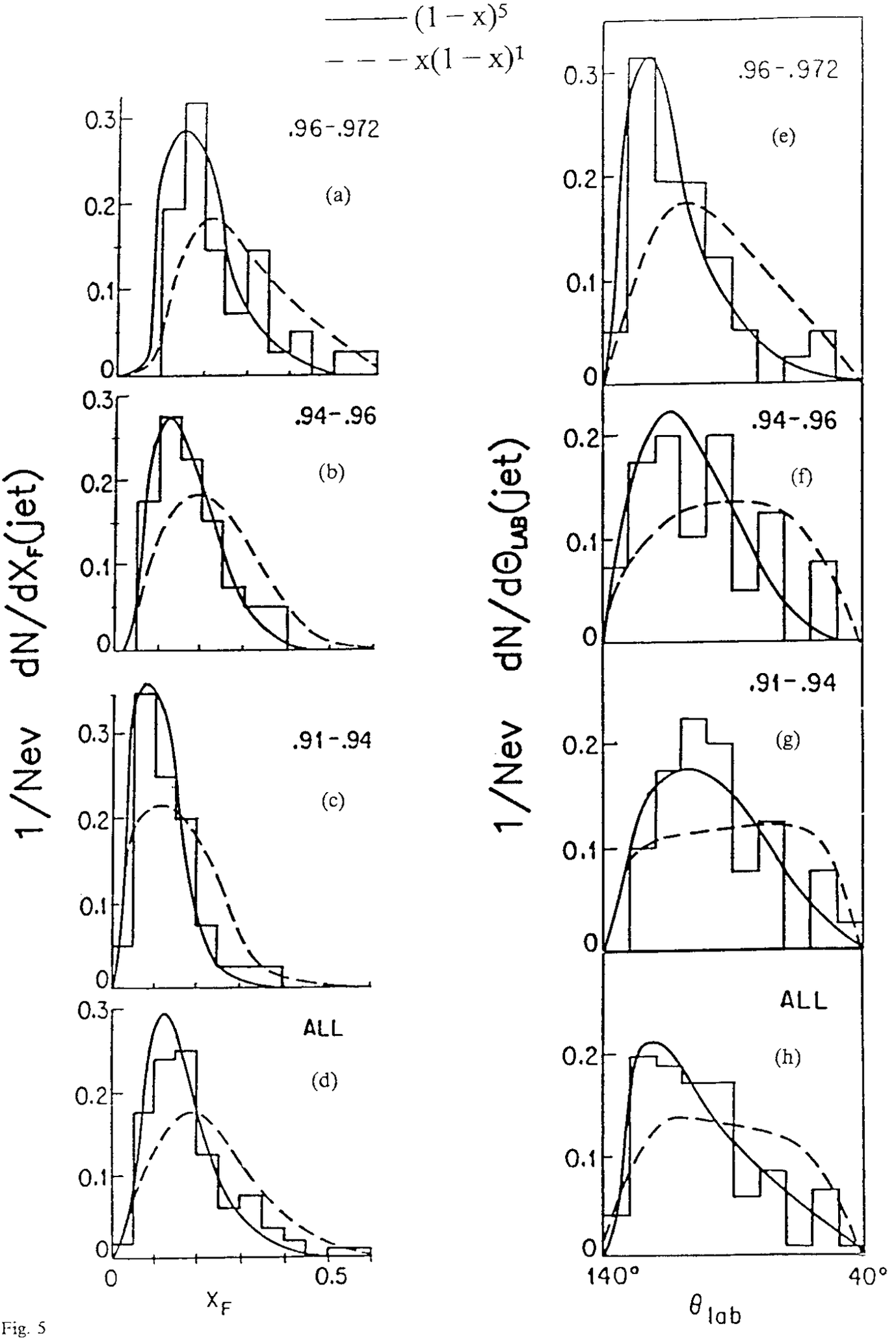
——— $(1-x)^5$
– – – $x(1-x)^1$
1/Nev dN/dX$_F$(jet)
.96-.972
(a)
.94-.96
(b)
.91-.94
(c)
ALL
(d)
0
0.5
X_F
1/Nev dN/dΘ_{LAB}(jet)
.96-.972
(e)
.94-.96
(f)
.91-.94
(g)
ALL
(h)
140°
40°
θ_{lab}

Fig. 5

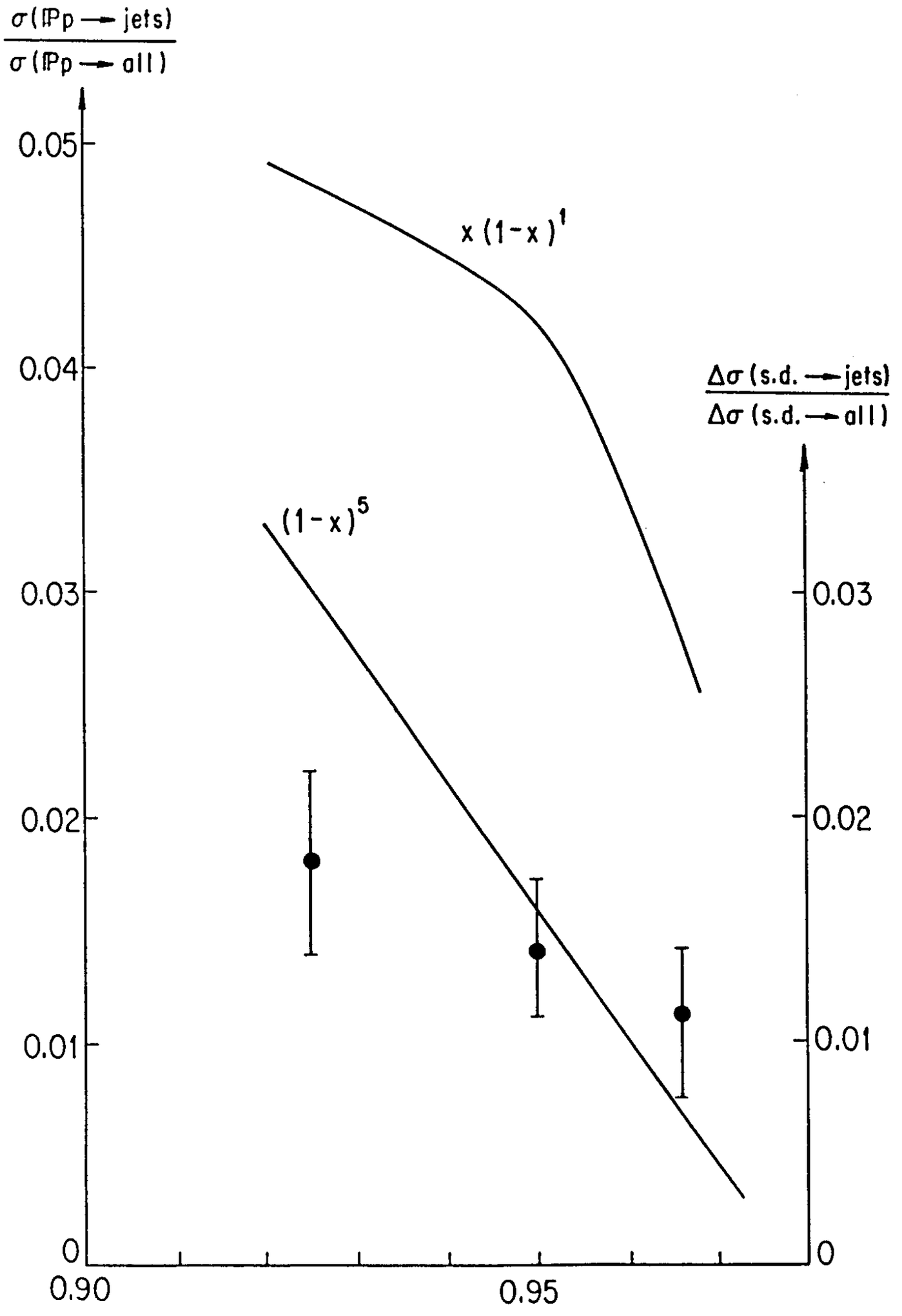
σ(ℙp → jets) / σ(ℙp → all)
0.05
0.04
0.03
0.02
0.01
0
x (1-x)¹
(1-x)⁵
Δσ (s.d. → jets) / Δσ (s.d. → all)
0.03
0.02
0.01
0
0.90
0.95
X proton

Fig. 6